Computational Journal of Mathematical and Statistical Sciences
4(1), 258–282
DOI:10.21608/cjmss.2025.342223.1090
https://cjmss.journals.ekb.eg/

Research article

A New Logarithmic Tangent-U Family of Distributions with Reliability Analysis in Engineering Data

Meshayil M. Alsolmi [1] *

[1] Department of Mathematics, College of Science and Arts at Khulis, University of Jeddah, Jeddah, Saudi Arabia

* **Correspondence:** mmralsulami@uj.edu.sa

Abstract: This article introduces a new family of distributions through the transformation involving tangent functions, referred to as the New Logarithmic Tangent-U family. The newly introduced family may be abbreviated as the NLT-U family of distribution. An overview of fundamental characteristics inherent to the proposed family of distributions is provided. We derived a special sub-model of the NLT-U family using the Weibull distribution as a baseline reference. This special model is termed the New Logarithmic Tangent-Weibull (NLT-Wei) distribution. The NLT-Wei distribution is very flexible and can be used to model data with hazard functions that exhibit increasing, decreasing, unimodal, increasing-decreasing-decreasing, and bathtub shapes. The Maximum Likelihood estimation scheme is employed to estimate the model parameters of the proposed family. A comprehensive Monte Carlo simulation analysis is conducted to assess the practical performance of the applied estimation method for the proposed family of distributions. The simulation experiment results show that biases and mean square errors decrease as sample sizes increase, even for smaller samples. Furthermore, the capability and applicability of the NLT-Wei distribution are illustrated by analyzing three real-world data sets from the engineering field. The suitability and flexibility of the NLT-Wei distribution are compared against several other distributions, including the Exponentiated Weibull, Kumaraswamy Weibull, New Generalized Logarithmic Weibull, Weibull, and Flexible Weibull distributions. The paper ends with a concluding discussion.

Keywords: New logarithmic tangent-U, Estimation, fundamental statistical properties, Monte Carlo simulation study, engineering data modeling.
Mathematics Subject Classification: 60E05; 62E10; 65C05
Received: 6 December 2024; Revised: 30 January 2025; Accepted: 2 February 2025; Online: 7 February 2025.

1. Introduction

Generally speaking, probability distributions have a pivotal role in modeling and analyzing random phenomena in every field of life. In the literature on distributions theory, there are several probability distributions for predicting and analyzing in various fields such as engineering (modeling reliability phenomena), education, healthcare/biomedical, economics (predicting and modeling export and import), actuarial/management, agronomy, genetics, and hydrology fields; for further detailed see, Alghamdi et al. [1], Tashkandy et al. [2], Alsadat et al. [3], and Gómez et al. [4]. But still, no specific probability distribution is available to handle every phenomenon because phenomena of real-world are complex. Therefore, this is the main reason to look forward to the development of more flexible probability distributions with greater distributional flexibility; see Odhah et al. [5]. The derivation of the new attractive methods to modify the existing distribution and improve its flexibility level is a prominent approach. Most of the new families of probability distribution which provide new probability distribution by the method of adding additional parameters. In the literature, several early and well-known distribution families have established by authors include the Exponentiated family introduced by Mudholkar and Srivastava [6], the Marshal-Olkin family introduced by Marshal and Olkin [7], the Exponentiated Exponential family introduced by Gupta and Kundu [8], the Beta-G family introduced by Eugene et al. [9], and the Kumaraswamy-G family of probability introduced by Nadarajah et al. [10].

Nowadays, the flexibility of existing distributions has been enhanced through the application of logarithmic and trigonometric functions, which give favorable aspects that improve the characteristics and adaptability of these distributions.

.

Using trigonometric and logarithmic functions, various methods of probability distributions were pioneered by the researchers in the existing literature. In this context, Chesneau et al. [11] presented a new approach of probability distributions using cosine and sine functions, while Souza et al. [12] developed the newly Sine-G class of probability distributions. Silveira et al. [13] projected the normal-tangent-G class, Alotaibi et al. [14] analyzed for the sine generalized linear exponential model under progressively censored, Nanga et al. [15] presented a tangent Topp-Leone family, Zaidi et al. [16] introduced Lomax tangent generalized family, Zhao et al. [17] introduced the Logarithmic-U family to enhance distribution flexibility, Ahmad et al. [18] derived the new cotangent Fréchet distribution, and Muhammad et al. [19] used a trigonometric function to propose the extended cosine-G family of probability distributions.

Recently, Alomair et al. [20] presented the Type-I Cosine Exponentiated-X family of lifetime distributions using a trigonometric function. The corresponding cumulative distribution function (CDF) for the newly introduced family is given by

$$G(w;\delta,\Omega) = \frac{e^{\cos\left(\frac{\pi}{2}\left\{1-(U(w;\Omega))^{\delta}\right\}\right)} - 1}{e-1}, \delta \in \mathrm{R}^{+}, w \in \mathrm{R}, \tag{1.1}$$

Where, $U(w;\Omega)$ is the CDF of any probability base model with parameter vectorΩ. Using Eq. (1.1), Alomair et al. [20] considered the CDF$U(w;\Omega)$ of the Weibull model and introduced a new distribution called a Type-I Cosine exponentiated Weibull distribution. Kamal et al. [21] presented the trigonometric Sine-G family of probability distributions. The CDF for this new trigonometric Sine-G

approach is given by

$$G(w;\delta,\Omega) = 1 - \frac{\delta\left(1-\sin\left(\frac{\pi}{2}U(w;\Omega)\right)\right)}{\delta-\sin\left(\frac{\pi}{2}U(w;\Omega)\right)}, \delta \in \mathrm{R}^{+}, w \in \mathrm{R}, \tag{1.2}$$

Where, $\delta \in \mathrm{R}^{+}$ is an extra parameter and$U(w;\Omega)$is the CDF of an existing model with parameter vector Ω.

Similarly, Benchiha et al. [22] introduced another trigonometric method called a new sine family of generalized distributions. For this novel sine family of generalized probability models, the CDF is provided by

$$G(w;\delta,\Omega) = \frac{\sin\left(\frac{\pi\delta}{2}U(w;\Omega)\right)}{\sin\left(\frac{\pi\delta}{2}\right)}, w \in \mathrm{R}, \tag{1.3}$$

where, $0 < \delta < 1$ and $U(w;\Omega)$is the CDF of any existing probability models with parameter vectorΩ. Using Eq. (1.3), Benchiha et al. [22] also enhanced the elasticity power of the Weibull distribution.

In this study, taking inspiration from the above discussion, we also introduce a novel trigonometric family of distributions by incorporating logarithmic and tangent functions with an additional parameter. This new family is called the New Logarithmic Tangent-U (NLT-U) family of distributions. Furthermore, the Weibull distribution is more popular in the distribution theory literature because it has properties of both the gamma and exponential distributions. Therefore, based on the newly proposed family, we derived an updated version of the Weibull distribution. Section 6 provides a comparison of the fitting performance of this newly introduced distribution with other existing distributions.

Definition: Let $u(w;\Omega)$be the probability density function (PDF) of any base distributions having the CDF $U(w;\Omega)$; that is$u(w;\Omega) = \frac{d}{dw}U(w;\Omega)$. Then the CDF $G(w;\delta,\Omega)$of the NLT-U family of distribution is given by

$$G(w;\delta,\Omega) = 1 - \frac{\log\left(e^{\delta}+\left(1-e^{\delta\tan\left(\frac{\pi}{4}U(w;\Omega)\right)}\right)\right)}{\delta}, \delta \in \mathrm{R}^{+}, w \in \mathrm{R}, \tag{1.4}$$

Where, $\delta \in \mathrm{R}^{+}$ is an extra (or additional) shape parameter and $U(w;\Omega)$is the CDF of any base probability model, depending on a parameter vector $\Omega \in \mathrm{R}$. For the NLT-U family, we need to verify whether the CDF is indeed valid or not. To address this, we present the following two propositions.

Preposition 1. For the CDF $G(w;\delta,\Omega)$of the NLT-U family, we will prove the following two conditions

$\lim_{w\to-\infty} G(w;\delta,\Omega) = 0$, and $\lim_{w\to\infty} G(w;\delta,\Omega) = 1$.

Proof. Link to Eq. (1.4), applying the limit, we have

$$\lim_{w\to-\infty} G(w;\delta,\Omega) = 1 - \frac{\log\left(e^{\delta}+\left(1-e^{\phi\tan\left(\frac{\pi}{4}U(-\infty;\Omega)\right)}\right)\right)}{\delta}, \tag{1.5}$$

if $U(w;\Omega)$is a real CDF of any baseline models, then

$U(-\infty;\Omega) = 0$, and $\tan(0) = 0$

$$\lim_{w\to-\infty} G(w;\delta,\Omega) = 1 - \frac{\log\left(e^{\delta}+\left(1-e^{0}\right)\right)}{\delta},$$

$$\lim_{w\to-\infty} G(w;\delta,\Omega) = 0.$$

Again, applying the limit of Eq. (1.4), we have

$$\lim_{w\to\infty} G(w;\delta,\Omega) = 1 - \frac{\log\left(e^{\delta} + \left(1 - e^{\phi\tan\left(\frac{\pi}{4}U(\infty;\Omega)\right)}\right)\right)}{\delta}, \tag{1.6}$$

As,$U(w;\Omega)$is surly a valid CDF of the baseline models, then
$U(\infty;\Omega) = 1$, and $\tan\left(\frac{\pi}{4}\right) = 1$

$$\lim_{w\to\infty} G(w;\delta,\Omega) = 1 - \frac{\log\left(e^{\delta} + \left(1 - e^{\delta}\right)\right)}{\delta},$$

After further simplification, we get

$$\lim_{w\to\infty} G(w;\delta,\Omega) = 1.$$

Proposition 2. The $G(w;\delta,\Omega)$ CDF is right continuous (non-negative) and differentiable.

Proof. $\frac{d}{dw}G(w;\delta,\Omega) = g(w;\delta,\Omega)$,

From the above discussion (i.e., propositions 1, and 2), it broadly proved that the CDF $G(w;\delta,\Omega)$in Eq. (1.4) of the NLT-U family of distributions is an actual (or valid) CDF and also very gorgeous. In the link to Eq. (1.4), the PDF$g(w;\delta,\Omega)$of the NLT-U family is presented by

$$g(w;\delta,\Omega) = \frac{\pi u(w;\Omega)\sec^2\left(\frac{\pi}{4}U(w;\Omega)\right)e^{\delta\tan\left(\frac{\pi}{4}U(w;\Omega)\right)}}{4\left(e^{\delta} + \left(1 - e^{\delta\tan\left(\frac{\pi}{4}U(w;\Omega)\right)}\right)\right)}, \tag{1.7}$$

Furthermore, linked to Eq. (1.4) and Eq. (1.7), the survival function (SF)$S(w;\delta,\Omega) = 1 - G(w;\delta,\Omega)$, hazard-function (HF)$h(w;\delta,\Omega) = \frac{g(w;\delta,\Omega)}{S(w;\delta,\Omega)}$, RHF (reverse HF) $\tau(w;\delta,\Omega) = \frac{g(w;\delta,\Omega)}{G(w;\delta,\Omega)}$, and CHF (cumulative HF) $H(w;\delta,\Omega) = -\log(S(w;\delta,\Omega))$ of the NLT-U method of distributions, respectively, are provided by the following

$$S(w;\delta,\Omega) = \frac{\log\left(e^{\delta} + \left(1 - e^{\delta\tan\left(\frac{\pi}{4}U(w;\Omega)\right)}\right)\right)}{\delta},$$

$$h(w;\delta,\Omega) = \frac{\pi\delta u(w;\Omega)\sec^2\left(\frac{\pi}{4}U(w;\Omega)\right)e^{\delta\tan\left(\frac{\pi}{4}U(w;\Omega)\right)}}{4\left\{\log\left(e^{\delta} + \left(1 - e^{\delta\tan\left(\frac{\pi}{4}U(w;\Omega)\right)}\right)\right)\right\}\left(e^{\delta} + \left(1 - e^{\delta\tan\left(\frac{\pi}{4}U(w;\Omega)\right)}\right)\right)},$$

$$\tau(w;\delta,\Omega) = \frac{\pi\delta u(w;\Omega)\sec^2\left(\frac{\pi}{4}U(w;\Omega)\right)e^{\delta\tan\left(\frac{\pi}{4}U(w;\Omega)\right)}}{4\left\{\delta - \log\left(e^{\delta} + \left(1 - e^{\delta\tan\left(\frac{\pi}{4}U(w;\Omega)\right)}\right)\right)\right\}\left(e^{\delta} + \left(1 - e^{\delta\tan\left(\frac{\pi}{4}U(w;\Omega)\right)}\right)\right)},$$

and

$$H(w;\delta,\Omega) = -\log\left(\frac{\log\left(e^{\delta} + \left(1 - e^{\delta\tan\left(\frac{\pi}{4}U(w;\Omega)\right)}\right)\right)}{\delta}\right).$$

In the following section, we introduce a logarithmic and trigonometric variant of the classical Weibull distribution (or model) based on the New Logarithmic Tangent-U (NLT-U) family. This new

distribution is termed the New Logarithmic Trigonometric Weibull (NLT-Wei) distribution. Section 3 derives some essential properties of the newly introduced probability family. In Section 4, we apply the well-known Maximum Likelihood Estimation method to estimate the unknown model parameters of the NLT-U method. Section 5 employs a Monte Carlo simulation analysis to evaluate the behavior of the estimators obtained through Maximum Likelihood Estimation. Section 6 assesses the practical performance of the NLT-U family using three real data sets from the engineering sector and compares the NLT-Wei model with other well-known classical distributions from the literature. Finally, Section 7 presents concluding remarks and a discussion.

2. NLT-Wei distribution

In the present section, we implement the derived method and propose a new logarithmic and trigonometric form of the traditional Weibull model. Let's suppose a RV (random variable)$W\,(\in \mathrm{R}^{+})$ follows the CDF $U\,(W;\Omega) = 1 - e^{-\phi w^{\beta}}$ and PDF $u\,(w;\Omega) = \phi\beta w^{\beta-1}e^{-\phi w^{\beta}}$ of the Weibull model with parameters $\phi > 0$, and $\beta > 0$, then the CDF $G\,(w;\delta,\Omega)$ of the NLT-Wei distribution is expressed by

$$G\,(w;\delta,\Omega) = 1 - \frac{\log\left(e^{\delta} + \left(1 - e^{\delta\tan\left(\frac{\pi}{4}\left(1-e^{-\phi w^{\beta}}\right)\right)}\right)\right)}{\delta}, w \geq 0, \tag{2.1}$$

Link to Eq. (2.1), the $S\,(w;\delta,\Omega)$SF of the NLT-Wei distribution is provided by

$$S\,(w;\delta,\Omega) = \frac{\log\left(e^{\delta} + \left(1 - e^{\delta\tan\left(\frac{\pi}{4}\left(1-e^{-\phi w^{\beta}}\right)\right)}\right)\right)}{\delta}, w \geq 0. \tag{2.2}$$

For the CDF $G\,(w;\delta,\Omega)$ and SF $S\,(w;\delta,\Omega)$of the NLT-Wei distribution, some graphical illustrations are visualized in Figure 1. These plots are gained for (i)δ =0.5, ϕ =3.6, β = 2.5 (blue curve line), (ii)δ =0.5, ϕ =0.7, β = 3.7 (red curve line), and (iii)δ = 3.9, ϕ = 0.7, β = 3.3 (green curve line). From Figure 1, it is visually confirmed that the CDF$G\,(w;\delta,\Omega)$ of the NLT-Wei distribution is a valid CDF.

Corresponding to Eq. (2.1) and Eq. (2.2), the PDF $g\,(w;\delta,\Omega)$, and $h\,(w;\delta,\Omega)$ HF of the NLT-Wei distribution are given, respectively, by

$$g\,(w;\delta,\Omega) = \frac{\pi\phi\beta w^{\beta-1}e^{-\phi w^{\beta}}\sec^{2}\left(\frac{\pi}{4}\left(1-e^{-\phi w^{\beta}}\right)\right)e^{\delta\tan\left(\frac{\pi}{4}\left(1-e^{-\phi w^{\beta}}\right)\right)}}{4\left(e^{\delta} + \left(1 - e^{\delta\tan\left(\frac{\pi}{4}\left(1-e^{-\phi w^{\beta}}\right)\right)}\right)\right)}, w > 0, \tag{2.3}$$

$$h\,(w;\delta,\Omega) = \frac{\pi\delta\phi\beta w^{\beta-1}e^{-\phi w^{\beta}}\sec^{2}\left(\frac{\pi}{4}\left(1-e^{-\phi w^{\beta}}\right)\right)e^{\delta\tan\left(\frac{\pi}{4}\left(1-e^{-\phi w^{\beta}}\right)\right)}}{4\left\{\log\left(e^{\delta} + \left(1 - e^{\delta\tan\left(\frac{\pi}{4}\left(1-e^{-\phi w^{\beta}}\right)\right)}\right)\right)\right\}\left(e^{\delta} + \left(1 - e^{\delta\tan\left(\frac{\pi}{4}\left(1-e^{-\phi w^{\beta}}\right)\right)}\right)\right)}, w > 0, \tag{2.4}$$

The PDF $g\,(w;\delta,\Omega)$and HF$h\,(w;\delta,\Omega)$ of the NLT-Wei model are also graphically visualized in Figure 2. The plots for PDF $g\,(w;\delta,\Omega)$are visualized with various parameter values are(i) δ = 0.3, ϕ =2.3, β =0.6 (blue curve line), (ii) δ = 0.1, ϕ =0.1, β =5.3 (red curve line), and (iii)δ = 0.2, ϕ =1.9, β =2.8 (green curve line), (iv) δ = 0.9, ϕ = 0.03, β = 5.9 (black curve line), and (v)δ = 0.3, ϕ = 5.3, β = 1.5 (violet curve line). From the plots (visual illustration) of the PDF in Figure 2, we can see that the

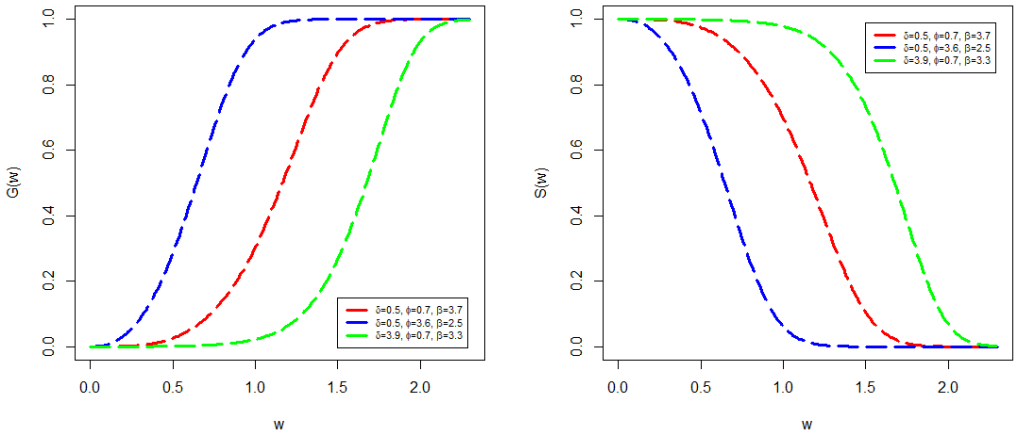

Figure 1. Visual illustration of CDF $G(w;\delta,\Omega)$ and SF $S(w;\delta,\Omega)$ of the NLT-Wei distribution.

PDF$g(w;\delta,\Omega)$ of FLT-Wei distribution has three behaviors lift skewed, symmetrical, and right skewed shape.

Likewise, the plots of HF $h(w;\delta,\Omega)$ of NLT-Wei distribution are gained with different parameter values. The parameter values are (i) δ =0.9, ϕ =0.1, β =2.7 (red curve line), (ii) δ =18.8, ϕ =7.2, β =0.5 (green curve line), (iii) δ =1.9, ϕ =2.3, β =0.1 (black curve line), (iv) δ =1.7, ϕ =1.4, β =0.7 (blue curve line), and (iv) δ =19.2, ϕ =9.2, β =0.6 (violet curve line). From the HF plots right penal in Figure 2, It is evident that the HF $h(w;\delta,\Omega)$of the NLT-Wei model exhibits the bathtub shape, unimodel, increasing-decreasing-increasing, decreasing, and increasing characteristics.

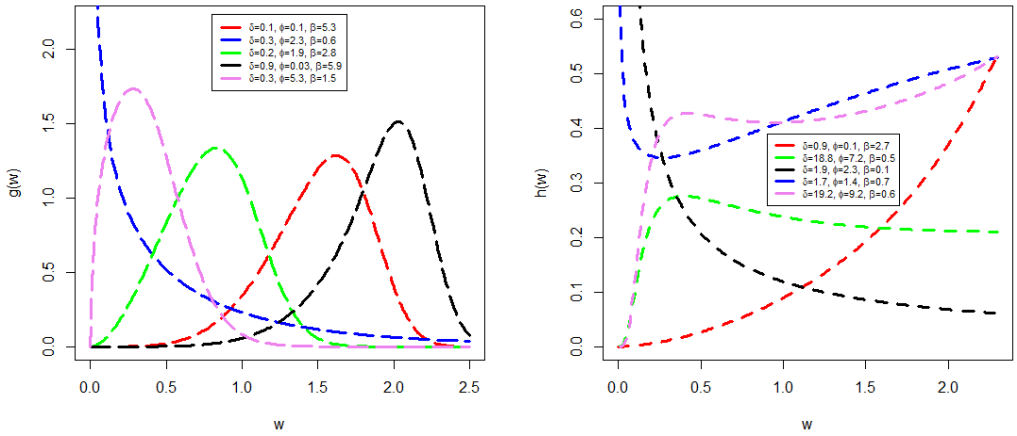

Figure 2. The $g(w;\delta,\Omega)$ and $h(w;\delta,\Omega)$ graphs of the NLT-Wei distribution.

Similarly, corresponding to Eq. (2.1), Eq. (2.2), and Eq. (2.3), the RHF $\tau(w;\delta,\Omega)$, and CHF $H(w;\delta,\Omega)$of the NLT-Wei distribution is presented by

$$\tau(w;\delta,\Omega)=\frac{\pi\delta\phi\beta w^{\beta-1}e^{-\phi w^{\beta}}\sec^{2}\left(\frac{\pi}{4}\left(1-e^{-\phi w^{\beta}}\right)\right)e^{\delta\tan\left(\frac{\pi}{4}\left(1-e^{-\phi w^{\beta}}\right)\right)}}{4\left(e^{\delta}+\left(1-e^{\delta\tan\left(\frac{\pi}{4}\left(1-e^{-\phi w^{\beta}}\right)\right)}\right)\right)\left\{\delta-\log\left(e^{\delta}+\left(1-e^{\delta\tan\left(\frac{\pi}{4}\left(1-e^{-\phi w^{\beta}}\right)\right)}\right)\right)\right\}},\ w>0,$$

and

$$H(w;\delta,\Omega)=-\log\left(\frac{\log\left(e^{\delta}+\left(1-e^{\delta\tan\left(\frac{\pi}{4}\left(1-e^{-\phi w^{\beta}}\right)\right)}\right)\right)}{\delta}\right),\ w>0.$$

Furthermore, let W be a random variable that follows the NLT-Wei distribution with $p\in(0,1)$, then the QF, say $Q_w(p)$can be expressed in the following form

$$Q_w(p)=\left[-\frac{1}{\phi}\log\left(1-\frac{4}{\pi}\tan^{-1}\left(\frac{\log\left(e^{\delta}-e^{(1-p)\delta}+1\right)}{\delta}\right)\right)\right]^{\frac{1}{\beta}}.$$

3. Statistical properties

Here, we originate some fundamental characteristics of the NLT-U family including the quantile function, quartiles, skewness, kurtosis, rth moments, and moment generating functions. The main purpose of these properties is to examine the features and nature of the proposed probability distribution such as the skewness is used to check the symmetry and asymmetry of the distribution. Likewise, kurtosis is generally used to measure the peakedness of the distribution such as mesokurtic, platykurtic, and leptokurtic of the distribution.

3.1. Quantile Function

If W follows the NLT-U family of distributions, then, the quartile function (QF), denoted as$Q(p)$, is given by

$$Q(p)=U^{-1}\left(\frac{4}{\pi}\tan^{-1}\left(\frac{\log\left(1-e^{\delta(1-p)}+e^{\delta}\right)}{\delta}\right)\right),\tag{3.1}$$

Proof. For $0<p<1$, the QF is the inverse of the CDF of the NLT-U method, that is

$$1-\frac{\log\left(e^{\delta}+\left(1-e^{\delta\tan\left(\frac{\pi}{4}\left(1-e^{-\phi w^{\beta}}\right)\right)}\right)\right)}{\delta}=p.$$

Hence

$$\frac{\log\left(e^{\delta}+\left(1-e^{\delta\tan\left(\frac{\pi}{4}U(w;\Omega)\right)}\right)\right)}{\delta}=(1-p),$$

Multiplying both sides by δ, we get

$$\log\left(e^{\delta}+\left(1-e^{\delta\tan\left(\frac{\pi}{4}U(w;\Omega)\right)}\right)\right)=\delta(1-p),$$

$$e^{\delta \tan\left(\frac{\pi}{4} U(w;\Omega)\right)} = \left(e^{\delta} - e^{\delta(1-p)} + 1\right),$$

Taking the logarithm, we get

$$U(w;\Omega) = \frac{4}{\pi} \tan^{-1} \frac{\log\left(e^{\delta} - e^{\delta(1-p)} + 1\right)}{\delta}.$$

Eq. (3.1) presents the quartile function (QF) of the NLT-U family of distributions in an explicit form, making it straightforward to generate random numbers from any updated version of the existing distributions.

The median (also known as the second quartile) of the NLT-U family of distributions is derived by replacing$p = 0.5$in Eq. (3.1), as presented by

$$Q(0.5) = U^{-1}\left(\frac{4}{\pi} \tan^{-1}\left(\frac{\log\left(1 - e^{\delta(0.5)} + e^{\delta}\right)}{\delta}\right)\right).$$

Furthermore, the 1^{st} and 3^{rd} quartile of the NLT-U family of probability distributions are computed by putting the values $p = 0.25$and $p = 0.75$in Eq. (3.1). Similarly, the 1^{st} and 3^{rd} quartiles of the NLT-U family are provided, respectively, by

$$Q(0.25) = U^{-1}\left(\frac{4}{\pi} \tan^{-1}\left(\frac{\log\left(1 - e^{\delta(0.25)} + e^{\delta}\right)}{\delta}\right)\right).$$

$$Q(0.75) = U^{-1}\left(\frac{4}{\pi} \tan^{-1}\left(\frac{\log\left(1 - e^{\delta(0.75)} + e^{\delta}\right)}{\delta}\right)\right).$$

Therefore, the Galton skewness (GASK) of the NLT-U family, say $GASK(w)$, is given by

$$GASK(w) = \frac{Q(0.75) - 2Q(0.5) + Q(0.25)}{Q(0.75) - Q(0.25)},$$

Where, the respective quantities $Q(0.25)$, $Q(0.5)$, and$Q(0.75)$are gained by inserting $p = 0.25$,$p = 0.5$, and $p = 0.75$, respectively in Eq. (3.1).

Similarly, the Moors kurtosis (MOKU) of the FLT-U family, say $MOKU(w)$, is given by

$$MOKU(w) = \frac{Q(0.875) - Q(0.625) - Q(0.125) + Q(0.375)}{Q(0.75) - Q(0.25)},$$

Where, the quantities$Q(0.125)$, $Q(0.25)$, $Q(0.375)$, $Q(0.625)$, $Q(0.75)$and$Q(0.875)$are gained by putting the values$p = (0.125, 0.25, 0.375, 0.625, 0.75, and 0.825)$, respectively, in Eq. (3.1).

3.2. Moments

Let W follow a random variable of the NLT-U family of distribution linked to the PDF$g(w;\delta,\Omega)$, then the r^{th} moment, say μ', is calculated by

$$\mu' = E(w^r) = \int_{-\infty}^{\infty} w^r g(w;\delta,\Omega)\ \partial w. \tag{3.2}$$

Now, by inserting Eq. (1.7) in Eq. (3.2), then we acquire

$$\mu' = E\left(w^r\right) = \int_{-\infty}^{\infty} w^r \frac{\pi u\left(w;\Omega\right)\sec^2\left(\frac{\pi}{4}U\left(w;\Omega\right)\right)e^{\delta\tan\left(\frac{\pi}{4}U(w;\Omega)\right)}}{4\left(e^{\delta}+\left(1-e^{\delta\tan\left(\frac{\pi}{4}U(w;\Omega)\right)}\right)\right)}\partial w,$$

$$\mu' = \int_{-\infty}^{\infty} w^r \frac{\pi}{4} e^{\delta} u\left(w;\Omega\right)\sec^2\left(\frac{\pi}{4}U\left(w;\Omega\right)\right)e^{\delta\tan\left(\frac{\pi}{4}U(w;\Omega)\right)}\left(1+e^{-\delta}\left(1-e^{\delta\tan\left(\frac{\pi}{4}\tan(w;\Omega)\right)}\right)\right)^{-1}\partial w. \tag{3.3}$$

Using the expansion $(1+w)^{-1} = \sum_{c=0}^{\infty}(-1)^c w^c$ and $(1-w)^c = \sum_{d=0}^{c}(-1)^d \binom{c}{d} w^d$.

Now, putting $w = e^{-\delta}\left(1-e^{\delta\tan\left(\frac{\pi}{4}U(w;\Omega)\right)}\right)$, and $w = e^{\delta\tan\left(\frac{\pi}{4}U(w;\Omega)\right)}$, respectively, in the above series, then, we get

$$\left(1+e^{-\delta}\left(1-e^{\delta\tan\left(\frac{\pi}{4}U(w;\Omega)\right)}\right)\right)^{-1} = \sum_{c=0}^{\infty}\sum_{d=0}^{c} e^{-c\delta}(-1)^{c+d}\binom{c}{d} e^{d\delta\tan\left(\frac{\pi}{4}U(w;\Omega)\right)}. \tag{3.4}$$

For more simplification, using Eq. (3.4) in Eq. (3.3)

$$\mu' = \frac{\pi}{4}\sum_{c=0}^{\infty}\sum_{d=0}^{c} e^{(1-c)\delta}(-1)^{c+d}\binom{c}{d}\int_{-\infty}^{\infty} w^r u\left(w;\Omega\right)\sec^2\left(\frac{\pi}{4}U\left(w;\Omega\right)\right)e^{(1+d)\delta\tan\left(\frac{\pi}{4}U(w;\Omega)\right)}\partial w. \tag{3.5}$$

Similarly, we also know that

$$e^{w} = \sum_{k=1}^{\infty}\frac{w^k}{k!}. \tag{3.6}$$

Using $w = (1-d)\,\delta\tan\left(\frac{\pi}{4}U\left(w;\Omega\right)\right)$ in Eq. (3.6), we obtain

$$e^{(1-d)\delta\tan\left(\frac{\pi}{4}U(w;\Omega)\right)} = \sum_{k=1}^{\infty}\frac{\left((1-d)\,\delta\tan\left(\frac{\pi}{4}U\left(w;\Omega\right)\right)\right)^k}{k!}. \tag{3.7}$$

Using Eq. (3.7), in Eq. (3.6), we get

$$\mu' = \frac{\pi}{4}\sum_{c=0}^{\infty}\sum_{d=0}^{c}\sum_{k=1}^{\infty}\frac{e^{(1-c)\delta}(-1)^{c+d}(1+d)^k\delta^k}{k!}\binom{c}{d}\Phi_{r,c,d,k}\left(w;\Omega\right), \tag{3.8}$$

where,

$$\Phi_{r,c,d,k}\left(w;\Omega\right) = \int_{-\infty}^{\infty} w^r u\left(w;\Omega\right)\sec^2\left(\frac{\pi}{4}U\left(w;\delta\right)\right)\left(\tan\left(\frac{\pi}{4}U\left(w;\Omega\right)\right)\right)^k\partial w.$$

Additionally, the NLT-U family of distributions' moment generating function (MGF), denoted as $M_w(t)$, is calculated as

$$M_w(t) = \int_{-\infty}^{\infty} e^{wt} g\left(w;\delta,\Omega\right)\,\partial w \tag{3.9}$$

By using exponential series$e^t = \sum_{r=0}^{\infty} \frac{t^r}{r!}$, and after putting Eq. (3.8)

$$M_w(t) = \sum_{r=0}^{\infty} \frac{t^r}{r!} \int_{-\infty}^{\infty} w^r g\left(w; \delta, \Omega\right) \partial w$$

$$M_w(t) = \frac{\pi}{4} \sum_{r=0}^{\infty} \sum_{c=0}^{\infty} \sum_{d=0}^{c} \sum_{k=1}^{\infty} \frac{e^{(1-c)\delta} (-1)^{c+d} (1+d)^k \delta^k w^r}{k! r!} \begin{pmatrix} c \\ d \end{pmatrix} \Phi_{r,c,d,k}\left(w; \Omega\right).$$

4. Estimation

In the present section, the model parameters of the NLT-U method are estimated by applying the maximum likelihood estimation (MLE) approach i.e. MLEs $\left(\hat{\delta}_{MLE}, \hat{\Omega}_{MLE}\right)$ of the parameters(δ, Ω). Let's suppose that a set of RS (random-samples) of size n, say $W_1, W_2, W_3, ...W_n$are taken from the proposed family with a PDF $g\left(w; \delta, \Omega\right)$. The then the likelihood-function (LF) associated with Eq. (1.7), is given by

$$T\left(\Theta / w_1, w_2, ...w_n\right) = \prod_{i=1}^{n} \frac{\pi u\left(w; \Omega\right) \sec^2\left(\frac{\pi}{4} U\left(w; \Omega\right)\right) e^{\delta \tan\left(\frac{\pi}{4} U(w;\Omega)\right)}}{4\left(e^{\delta} + \left(1 - e^{\delta \tan\left(\frac{\pi}{4} U(w;\Omega)\right)}\right)\right)}. \tag{4.1}$$

Where $\Theta = (\delta, \Omega)^T$. The log LF (LLF), say$\ell\left(\Theta\right)$, is given by

$$\begin{array}{c} \ell\left(\Theta\right) = n \log \pi - n \log 4 + \sum_{i=1}^{n} \log u\left(w_i; \Omega\right) + \sum_{i=1}^{n} \log \sec^2(\frac{\pi}{4} U\left(w_i; \Omega\right) \\ +\delta \sum_{i=1}^{n} \tan(\frac{\pi}{4} U\left(w_i; \Omega\right) \ - \sum_{i=1}^{n} \log \left\{e^{\delta} + \left(1 - e^{\delta \tan(\frac{\pi}{4} U(w_i;\Omega)}\right)\right\} \end{array}. \tag{4.2}$$

Link to Eq. (4.2), taking derivative W.R.T $\delta$and Ω, are respectively given by

$$\frac{\partial}{\partial \delta} \ell\left(\Theta\right) = \sum_{i=1}^{n} \tan(\frac{\pi}{4} U\left(w_i; \Omega\right) \ - \sum_{i=1}^{n} \frac{\partial\left(e^{\delta} + \left(1 - e^{\delta \tan(\frac{\pi}{4} U(w_i;\Omega)}\right)\right) \Big/ \partial \delta}{\left(e^{\delta} + \left(1 - e^{\delta \tan(\frac{\pi}{4} U(w_i;\Omega)}\right)\right)},$$

and

$$\begin{array}{c} \frac{\partial}{\partial \Omega} \ell\left(\Theta\right) = \sum_{i=1}^{n} \frac{\partial u(w_i;\Omega)/\partial \Omega}{u(w_i;\Omega)} - \sum_{i=1}^{n} \frac{\pi}{4} \frac{\tan(\frac{\pi}{4} U(w_i;\Omega) \partial U(w_i;\Omega)/\partial \Omega}{\sec^2(\frac{\pi}{4} U(w_i;\Omega)} \\ +\delta \sum_{i=1}^{n} \frac{\pi}{4} \frac{\sec^2(\frac{\pi}{4} U(w_i;\Omega) \partial U(w_i;\Omega)/\partial \Omega}{\tan(\frac{\pi}{4} U(w_i;\Omega)} - \sum_{i=1}^{n} \frac{\partial\left(e^{\delta} + \left(1 - e^{\delta \tan(\frac{\pi}{4} U(w_i;\Omega)}\right)\right) \Big/ \partial \Omega}{\left(e^{\delta} + \left(1 - e^{\delta \tan(\frac{\pi}{4} U(w_i;\Omega)}\right)\right)} \end{array},$$

Setting$\frac{\partial}{\partial \delta} \ell\left(\Theta\right) = 0$, and $\frac{\partial}{\partial \Omega} \ell\left(\Theta\right) = 0$, and solving simultaneously, we get MLEs $\left(\hat{\delta}, \hat{\Omega}\right)$ of (δ, Ω).

5. Simulations

In the present section, we use the Monte-Carlo-Simulation study (MCSS) to judge the performance (or estimator's behaviors) of the NLT-Wei distribution i.e., MLEs$\left(\hat{\delta}_{MLE}, \hat{\phi}_{MLE}, \hat{\beta}_{MLE}\right)$. For random number generation, the inverse of the CDF of the NLT-Wei distribution is used. Four sets of different parameter values are employed and MCSS is carried out. Four sets of parameters combination are: Set I(δ, ϕ, β):(1.3, 0.9, 4.1), Set II(δ, ϕ, β): (1.6, 3.8, 1.2), Set III(δ, ϕ, β): (1.5, 1.7, 0.9), and Set IV(δ, ϕ, β):

(4.6, 0.8, 2.5). Typically, simulation studies use predefined (or default) parameter values. The parameter range for the NLEP-Weibull distribution, with $\delta\,(\delta \in \mathrm{R}^{+})$, $\phi\,(\phi \in \mathrm{R}^{+})$, and $\beta\,(\beta \in \mathrm{R}^{+})$ has already been stated in this article. As a result, for the numerical process of the simulation study, we can take any values for δ, ϕ, and β within their specified ranges. RS of sizes 25, 50, 75, 100, 200, 300, 400, 500, 600, 700, 800, 900, and 1000 generated from NLT-Wei distribution are used in the simulation analysis. For each setting (or group) of parameter values, the process is repeated N=1000 times, and the average of estimated parameter values, biases, and MSE are obtained for each parameter (i.e., δ, ϕ, and β). To assess the effectiveness of the applied statistical techniques$\left(\hat{\delta}_{MLE}, \hat{\phi}_{MLE}, \hat{\beta}_{MLE}\right)$, performance metrics like mean square errors (MSEs), biases, and average values of MLEs are utilized. The simulation process is conducted by using R language software (Core Team, 2023, version 4.2.3) with the root solve package. The statistical tools with mathematical expression, respectively, given by

$$Bias\,(\Xi) = \frac{1}{N}\sum_{i=1}^{N}(\hat{\Xi} - \Xi),$$

and

$$MSE\,(\Xi) = \frac{1}{N}\sum_{i=1}^{N}(\hat{\Xi} - \Xi)^2,$$

where, $\Xi = (\delta, \phi, \beta)$.

For set I(δ, ϕ, β), and set II (δ, ϕ, β), the numerical values of the simulation analysis are recorded in Table 1 and graphically illustrated in Figures 3, and 4. Similarly, for set III(δ, ϕ, β), and set IV (δ, ϕ, β), the numerical values are listed in Table 2 and visually illustrated in Figures 5, and 6. From Tables 1 and 2, it is demonstrated that the Biases$\left(\hat{\delta}_{MLE}, \hat{\phi}_{MLE}, \hat{\beta}_{MLE}\right)$, and the MSEs$\left(\hat{\delta}_{MLE}, \hat{\phi}_{MLE}, \hat{\beta}_{MLE}\right)$are decline (decrease to zero), whereas the average estimate values are near to true (or exact) values as the sample size increases (i.e.,$n \to \infty$). Similarly, from the graphical illustration (i.e., Figures 3,4,5,6), it is also observed that the MSEs of the $\hat{\delta}_{MLE}$, $\hat{\phi}_{MLE}$, and $\hat{\beta}_{MLE}$, and the Biases of the $\hat{\delta}_{MLE}$, $\hat{\phi}_{MLE}$, and $\hat{\beta}_{MLE}$ are gradually declining to zero while the estimated values (i.e., MLEs) are constantly stable as the sample size increases. From the numerical and graphical illustration, we observed (or examined) that the MLEs $\left(\hat{\delta}_{MLE}, \hat{\phi}_{MLE}, \hat{\beta}_{MLE}\right)$ of the NLT-Wei model are consistent estimators.

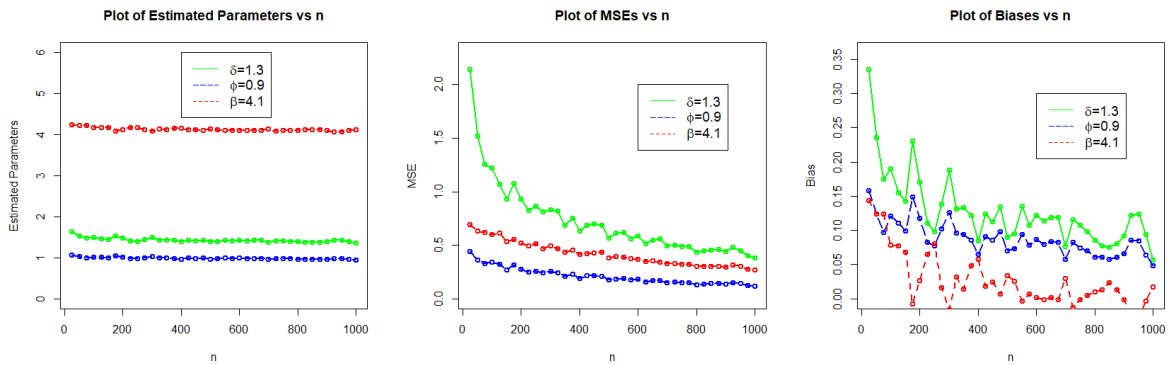

Figure 3. The visual representation (simulation results) for set I (δ, ϕ, β).

Table 1. The simulation results of the NLT-Wei model for Sets I(δ, ϕ, β), and II(δ, ϕ, β).

		Set I			Set II		
		$\delta = 1.3, \phi = 0.9, \beta = 4.1$			$\delta = 1.6, \phi = 3.8, \beta = 1.2$		
n	Est.	MLE	MSE	Bias	MLE	MSE	Bias
25	$\hat{\delta}$	1.63519	2.14475	0.33519	1.26639	1.36446	-0.33361
	$\hat{\phi}$	1.05769	0.44345	0.15768	3.61791	1.14279	-0.18208
	$\hat{\beta}$	4.24367	0.69119	0.14367	1.46793	0.27331	0.26792
50	$\hat{\delta}$	1.53634	1.51806	0.23634	1.30441	1.22472	-0.29558
	$\hat{\phi}$	1.02346	0.36313	0.12346	3.55946	1.12814	-0.24054
	$\hat{\beta}$	4.22427	0.63499	0.12427	1.39891	0.17948	0.19891
75	$\hat{\delta}$	1.47446	1.25377	0.17446	1.45855	1.09896	-0.14145
	$\hat{\phi}$	0.99746	0.33169	0.09746	3.67555	0.98203	-0.12445
	$\hat{\beta}$	4.22384	0.61816	0.12385	1.33597	0.13037	0.13597
100	$\hat{\delta}$	1.49003	1.22278	0.19003	1.4147	1.0438	-0.18529
	$\hat{\phi}$	1.02063	0.34123	0.12063	3.63355	0.95376	-0.16644
	$\hat{\beta}$	4.17789	0.59765	0.07789	1.33638	0.12073	0.13638
200	$\hat{\delta}$	1.47109	0.93053	0.17109	1.50426	0.84958	-0.09573
	$\hat{\phi}$	1.01734	0.27788	0.11734	3.70115	0.78472	-0.09885
	$\hat{\beta}$	4.12641	0.52218	0.02641	1.29142	0.08189	0.09142
300	$\hat{\delta}$	1.48788	0.83324	0.13152	1.55732	0.69218	-0.04268
	$\hat{\phi}$	1.02649	0.25779	0.09583	3.75563	0.64725	-0.04437
	$\hat{\beta}$	4.0841	0.49141	0.03197	1.25956	0.06214	0.05956
400	$\hat{\delta}$	1.38457	0.63486	0.08457	1.5811	0.6661	-0.01889
	$\hat{\phi}$	0.96466	0.19117	0.06466	3.7807	0.617	-0.0193
	$\hat{\beta}$	4.15765	0.41776	0.05766	1.25214	0.05457	0.05214
500	$\hat{\delta}$	1.39017	0.56576	0.09017	1.58991	0.57538	-0.01009
	$\hat{\phi}$	0.96972	0.17701	0.06972	3.79583	0.53392	-0.00417
	$\hat{\beta}$	4.13371	0.38496	0.03371	1.24109	0.04616	0.04109
600	$\hat{\delta}$	1.42187	0.58632	0.12187	1.59547	0.54501	-0.00453
	$\hat{\phi}$	0.98712	0.18439	0.08712	3.79576	0.4971	-0.00423
	$\hat{\beta}$	4.10194	0.36584	0.00195	1.24042	0.0434	0.04043
700	$\hat{\delta}$	1.3765	0.49739	0.0765	1.58916	0.47604	-0.01083
	$\hat{\phi}$	0.95748	0.15131	0.05748	3.78464	0.44736	-0.01536
	$\hat{\beta}$	4.13001	0.32889	0.03001	1.23684	0.03587	0.03684
800	$\hat{\delta}$	1.38581	0.43234	0.08581	1.61483	0.4453	0.01483
	$\hat{\phi}$	0.96073	0.13163	0.06073	3.81152	0.41469	0.01152
	$\hat{\beta}$	4.10973	0.30401	0.00973	1.22625	0.03205	0.02625
900	$\hat{\delta}$	1.39169	0.43955	0.09169	1.61937	0.42063	0.01937
	$\hat{\phi}$	0.96609	0.13799	0.06609	3.81702	0.39146	0.01702
	$\hat{\beta}$	4.09845	0.29768	-0.00154	1.22199	0.02954	0.02199
1000	$\hat{\delta}$	1.35666	0.38084	0.05666	1.60106	0.40071	0.00106
	$\hat{\phi}$	0.94796	0.11645	0.04796	3.79804	0.37524	-0.00195
	$\hat{\beta}$	4.11777	0.27067	0.01778	1.22421	0.02861	0.02422

Table 2. The simulation results of the NLT-Wei model for Sets III(δ, ϕ, β), and IV(δ, ϕ, β).

		Set I			Set II		
		$\delta = 1.5, \phi = 1.7, \beta = 0.9$			$\delta = 4.6, \phi = 0.8, \beta = 2.5$		
n	Est.	MLE	MSE	Bias	MLE	MSE	Bias
25	$\hat{\delta}$	1.40312	2.00697	-0.09688	4.03946	2.30881	-0.56054
	$\hat{\phi}$	1.62713	0.88745	-0.07287	0.64368	0.15461	-0.15632
	$\hat{\beta}$	1.06293	0.12066	0.16293	2.94723	0.77709	0.44723
50	$\hat{\delta}$	1.4198	1.78325	-0.08019	4.03739	2.12797	-0.56261
	$\hat{\phi}$	1.66081	0.81476	-0.03919	0.66852	0.12419	-0.13147
	$\hat{\beta}$	1.01602	0.08206	0.11602	2.84859	0.59454	0.34859
75	$\hat{\delta}$	1.46994	1.57211	-0.03005	4.02197	2.13113	-0.57802
	$\hat{\phi}$	1.68986	0.78089	-0.01014	0.66789	0.11457	-0.13211
	$\hat{\beta}$	0.99128	0.07231	0.09129	2.83922	0.57217	0.33922
100	$\hat{\delta}$	1.43283	1.41423	-0.06716	4.11101	1.82084	-0.48899
	$\hat{\phi}$	1.67873	0.70709	-0.02127	0.68548	0.09342	-0.11452
	$\hat{\beta}$	0.98928	0.0672	0.08928	2.77348	0.42974	0.27348
200	$\hat{\delta}$	1.5187	1.10338	0.0187	4.14001	1.57792	-0.45998
	$\hat{\phi}$	1.72848	0.55733	0.08482	0.70045	0.07582	-0.09955
	$\hat{\beta}$	0.95074	0.04314	0.05074	2.719	0.33011	0.219
300	$\hat{\delta}$	1.52239	0.92526	0.02239	4.34659	0.92365	-0.2534
	$\hat{\phi}$	1.73002	0.47226	0.03003	0.74647	0.047	-0.05353
	$\hat{\beta}$	0.93942	0.03518	0.03942	2.61958	0.17586	0.11958
400	$\hat{\delta}$	1.50677	0.75234	0.00677	4.27695	1.01122	-0.32305
	$\hat{\phi}$	1.71353	0.38689	0.01353	0.72855	0.04933	-0.07145
	$\hat{\beta}$	0.93701	0.02834	0.03701	2.63776	0.17601	0.13776
500	$\hat{\delta}$	1.51153	0.60977	0.01154	4.37826	0.67646	-0.22174
	$\hat{\phi}$	1.71563	0.31412	0.01564	0.74739	0.03468	-0.0526
	$\hat{\beta}$	0.92802	0.02365	0.02802	2.59129	0.09612	0.09129
600	$\hat{\delta}$	1.52338	0.61224	0.02338	4.3927	0.65203	-0.20729
	$\hat{\phi}$	1.72397	0.31383	0.02397	0.75355	0.03195	-0.04645
	$\hat{\beta}$	0.92565	0.0223	0.02566	2.58522	0.09987	0.08522
700	$\hat{\delta}$	1.47777	0.49068	-0.02222	4.4424	0.53062	-0.15759
	$\hat{\phi}$	1.6925	0.25849	-0.07499	0.76197	0.02609	-0.03803
	$\hat{\beta}$	0.92914	0.01974	0.02914	2.56907	0.07407	0.06908
800	$\hat{\delta}$	1.49136	0.45372	0.01538	4.40068	0.5812	-0.19931
	$\hat{\phi}$	1.69879	0.23952	0.01871	0.75271	0.02756	-0.04729
	$\hat{\beta}$	0.92532	0.01743	0.01972	2.58102	0.08977	0.08102
900	$\hat{\delta}$	1.49288	0.39607	-0.00712	4.47396	0.40404	-0.12604
	$\hat{\phi}$	1.69914	0.20878	-0.08513	0.77303	0.02065	-0.02696
	$\hat{\beta}$	0.92266	0.01507	0.02266	2.54582	0.04484	0.04582
1000	$\hat{\delta}$	1.46983	0.36851	-0.03017	4.49305	0.34056	-0.10695
	$\hat{\phi}$	1.68524	0.19596	-0.01476	0.77487	0.01766	-0.02512
	$\hat{\beta}$	0.92349	0.01413	0.02349	2.54158	0.03555	0.04158

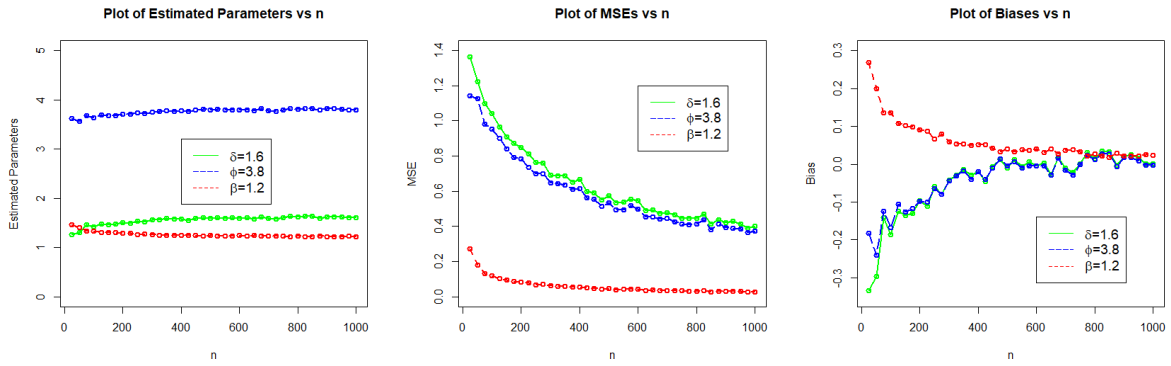

Figure 4. The visual representation (simulation results) for set II (δ, ϕ, β).

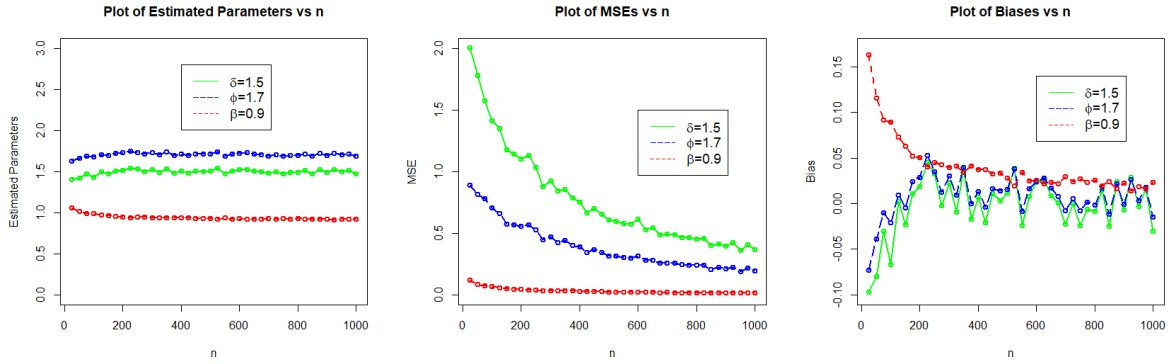

Figure 5. The visual representation (simulation results) for set III (δ, ϕ, β).

6. Real Data Analysis

In this section of the article, three real data sets (for illustrative purposes) are chosen from the engineering sector to demonstrate the efficacy and applicability of the NLT-Wei distribution compared to other existing distributions. The first illustration (numerically as well as graphically) of the NLT-Wei distribution is based on the data set representing the failure time of electronic devices (onward represented by DS 1) and taken from Chamunorwa et al. [27]. The second illustration of the NLT-Wei distribution is based on the data sets representing the strengths of 1.5 cm glass fibers (onward represented by DS 2) and taken from the paper of Dey et al. [28]. Similarly, the third illustration of the NLT-Wei model is also based on the data set from the engineering sector, which includes impregnated 1000-carbon fiber tows and single-carbon fibers (onward represented by DS 3) and taken from the research paper of Nagarjuna et al. [29].

We apply the NLT-Wei distribution to each data set to evaluate its flexibility and performance compared to other existing distributions. These include the Exponentiated-Weibull (E-Wei) distribution proposed by Mudholkar and Srivastava [6], the Kumaraswamy-Weibull (K-Wei) distribution introduced by Cordeiro et al. [23], the classical Weibull model developed by Weibull [24], the Flexible Weibull (F-Wei) distribution developed by Bebbington et al. [25], and the New Generalized Logarithmic Weibull (NGL-Wei) distributions suggested by Shah et al. [26]. The CDFs of the E-Wei, K-Wei, classical Wei, E-Wei, F-Wei, and NGL-Wei models are given by

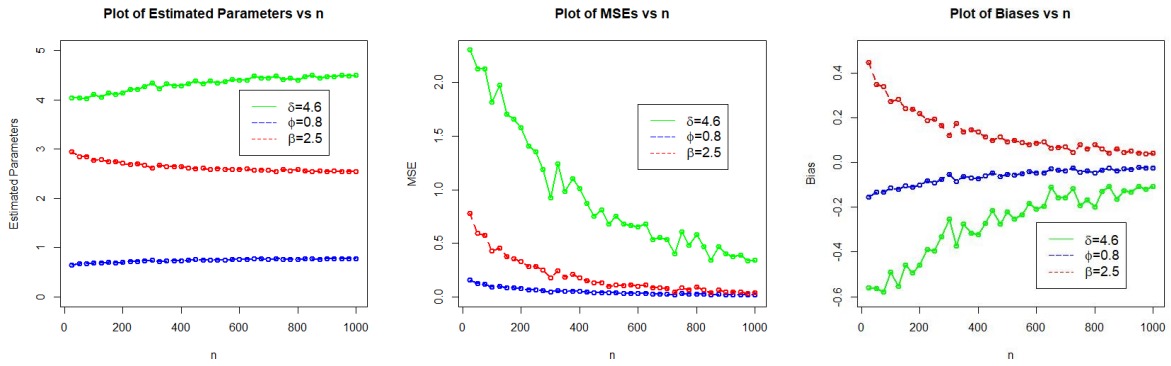

Figure 6. The visual representation (simulation results) for set IV (δ, ϕ, β).

$$G(w;\delta,\Omega) = \left(1 - e^{-\phi w^{\beta}}\right)^{\delta}, w \in \mathrm{R}^{+},$$

$$G(w;a,b,\phi,\beta) = 1 - \left[1 - \left(1 - e^{-\phi w^{\beta}}\right)^{a}\right]^{b}, w \in \mathrm{R}^{+},$$

$$G(w;\phi,\beta) = 1 - e^{-\phi w^{\beta}}, w \in \mathrm{R}^{+},$$

$$G(w;\phi,\beta) = 1 - e^{-e^{\left(\phi w - \frac{\beta}{w}\right)}}, w \in \mathrm{R}^{+},$$

And

$$G(w;\delta,\phi,\beta) = \frac{e^{\delta}\left(1 - e^{-\phi w^{\beta}}\right)}{\left(e - \log\left(1 - e^{-\phi w^{\beta}}\right)\right)^{\delta}}, w \in \mathrm{R}^{+},$$

respectively, where$\delta > 0$,$\phi > 0$,$\beta > 0$,$b > 0$, and $a > 0$.

After choosing existing Weibull distributions as competing distributions, now we go forward with analytical measures (or information criteria (IC)) along with P-values to identify more optimal distributions among the NLT-Wei and other competing distributions. These analytical measures chosen as comparative tools include the (I) Akaike IC (AIC), (II) Bayesian IC (BIC), (III) Consistent Akaike IC (CAIC), (IV) Hannan-Quinn IC (HQIC), (V) Cramer von Mises (CRMI), (VI) Anderson-Darling (ANDA), and (VII) Kolmogorov-Smirnov (KOSM). The mathematical expression of these analytical measures, respectively, are given by

$$AIC = 2k - 2\ell(\Theta),$$

$$BIC = k\log(n) - 2\ell(\Theta),$$

$$CAIC = \frac{2kn}{k - n - 1} - 2\ell(\Theta),$$

$$HQIC = 2k\log\left[\log(n)\right] - 2\ell(\Theta),$$

$$CRMI = \sum_{i=1}^{n}\left(G\left(w_i\right) - \frac{2i-1}{2n}\right)^2 + \frac{1}{12n}, ANDA = -n - \frac{1}{n}\sum_{i=1}^{n}(2i-1)\times\left[\log\left(1 - G\left(w_{(i-n+1)}\right)\right) + \log\left(G\left(w_{(i)}\right)\right)\right],$$

and

$$KOSM = \underset{i=1,2,3...n}{Max}\left(\left(\frac{i}{n} - G\left(w_{(i)}\right)\right), \left(G\left(w_{(i)}\right) - \frac{i-1}{n}\right)\right),$$

In the above mathematical expression, k represent parameter numbers n represent the sample size, and $\ell\left(\Theta\right)$represent LLF. The values of MLEs and analytical measures are carried (or found) out via R computer software with the **AdquacyModel** package and BFGS algorithm. Generally, if a distribution among the competitive distributions that have minimum values of these analytical (model selection criteria) measures and maximum P-value then it will be a good competitor for the respective data set.

6.1. Application I

.

In this sub-section, we offer the first comparison of the NLT-Wei distribution with other competing distributions by using DS 1. The DS 1 represents the failure time of electronic devices and for reader interest, the DS1 is given by: 7.89, 4.69, 4.20, 3.34, 3.03, 3.03, 2.33, 2.17, 2.14, 2.05, 2.02, 1.81, 1.80, 1.80, 1.64, 1.63, 1.60, 1.58, 1.55, 1.54, 1.54, 1.53, 1.52, 1.51, 1.50, 1.45, 1.43, 1.40, 1.34, 1.33, 1.31, 1.29, 1.20,1.18, 1.15, 1.11, 1.10, 1.10, 1.05, 1.03, 1.02, 1.01, 1.00, 0.99, 0.95, 0.92, 0.90, 0.85, 0.83, 0.80, 0.80, 0.79, 0.79, 0.73, 0.72, 0.72, 0.72, 0.68, 0.67, 0.65, 0.63, 0.60, 0.60, 0.56, 0.54, 0.52, 0.43, 0.42, 0.40, 0.38, 0.36, 0.35, 0.34, 0.29, 0.24, 0.24, 0.23, 0.20, 0.19, 0.18, 0.13, 0.12, 0.11, 0.11, 0.10, 0.10, 0.09, 0.09, 0.08, 0.07, 0.07, 0.06, 0.05, 0.04, 0.03, 0.03, 0.02, 0.02, 0.02, 0.01, 0.01.

Some key measures for DS 1 are: min.=0.01, median=0.8, mean=1.025, Q_1 (1^{st} quartile). =0.24, Q_3 (3^{rd} quartile). =1.450, max.=7.89, skewness=3.0017, kurtosis=16.7089, variance=1.2529, and range=7.88. Additionally, for DS 1, the Box plot, Violin-plot, and TTT-plot are sketched in Figure 7.

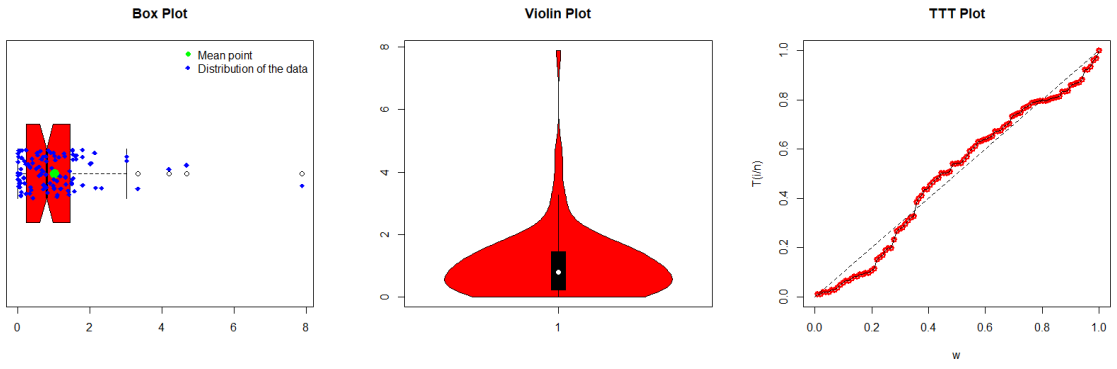

Figure 7. The Box, Violin, and TTT plots of the DS 1.

Link to DS 1, the values of MLEs of the fitted distributions (i.e. $\hat{\delta}_{MLE}$, $\hat{\phi}_{MLE}$, $\hat{\beta}_{MLE}$, $\hat{a}_{MLE}$, and $\hat{b}_{MLE}$) are recorded in Table 3. Furthermore, Figure 8 illustrates the profile log-likelihood function plots of

$\hat{\delta}_{MLE}$, $\hat{\phi}_{MLE}$, and $\hat{\beta}_{MLE}$of the NLT-Wei distribution. From Figure 8, we can clearly see that the estimated parameters are maximization of the Log-LF of the NLT-Wei distribution.

Using DS 1, the AIC, BIC, CAIC, HQAIC, CRMI, ANDA, KOSA, and P-Values of the NLT-Wei and competing distributions are reported in Table 3. For the NLT-Wei distribution, these values are AIC=209.1255, BIC=216.9709, CAIC=209.3729, HQIC=212.3015, CRMI=0.1086, ANDA=0.6864, KOSA=0.0646, and P= 0.7930. Thus, Table 4, categorically confirms that the AIC, BIC, CAIC, HQAIC, CRMI, ANDA, and KOSA values are the minimum of the NLT-Wei distribution and have a higher P-value than the other compared distribution for DS 1. Therefore, it is concluded that the NLT-Wei distribution provides the first-ranked fit to the DS 1. Similarly, supporting numerical results recorded in Table 4, we also show the graphical illustration of the NLT-Wei distribution for DS 1. For graphical illustration, we select the estimated PDFs, and estimated CDFs of the fitted distributions; see Figure 9. From Figure 9, we can also see the close-fitting ability of the NLT-Wei distribution as compared to the other competitive distributions.

Table 3. For DS 1, the values$\hat{\delta}_{MLE}$, $\hat{\phi}_{MLE}$, $\hat{\beta}_{MLE}$, $\hat{a}_{MLE}$, and $\hat{b}_{MLE}$.

Models	$\hat{\delta}_{MLE}$	$\hat{\phi}_{MLE}$	$\hat{\beta}_{MLE}$	$\hat{a}_{MLE}$	$\hat{b}_{MLE}$
FLT-Wei	0.8322	1.8840	0.7354	–	–
E-Wei	0.7929	0.8113	1.0604	–	–
K-Wei	–	3.2678	1.0341	0.7313	0.2728
NGL-Wei	-0.1478	0.9681	0.9464	–	–
Wei	–	1.0094	0.9259	–	–
F-Wei	–	0.3297	0.0826	–	–

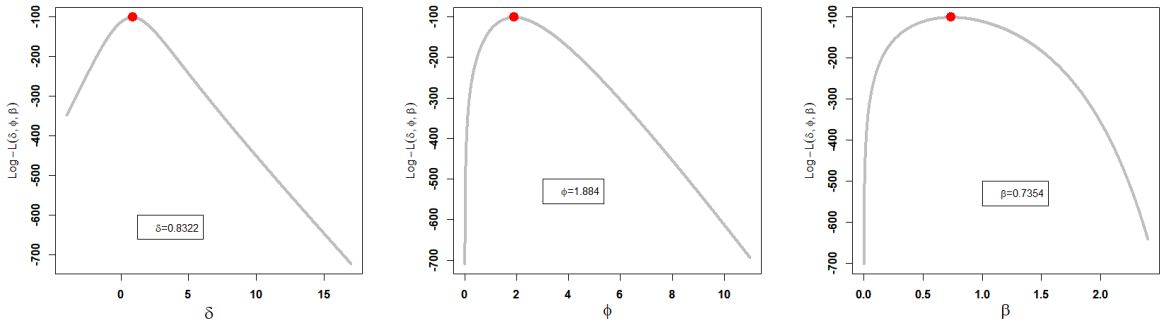

Figure 8. The profile log-likelihood plots for $\hat{\delta}_{MLE}$, $\hat{\phi}_{MLE}$, and$\hat{\beta}_{MLE}$of the FLT-Wei model using DS 1.

6.2. Application II

In this second subsection, we provide a comparison of the NLT-Wei distribution with other competing models using DS 2. This data set represents the strengths of 1.5 cm glass fibers, originally collected by researchers at the UK National-Physical-Laboratory and for reader interest, the DS2 is given by: 0.55, 0.74, 0.77, 0.81, 0.84,0.93, 1.04, 1.11, 1.13, 1.24, 1.25, 1.27, 1.28, 1.29, 1.30, 1.36, 1.39, 1.42,

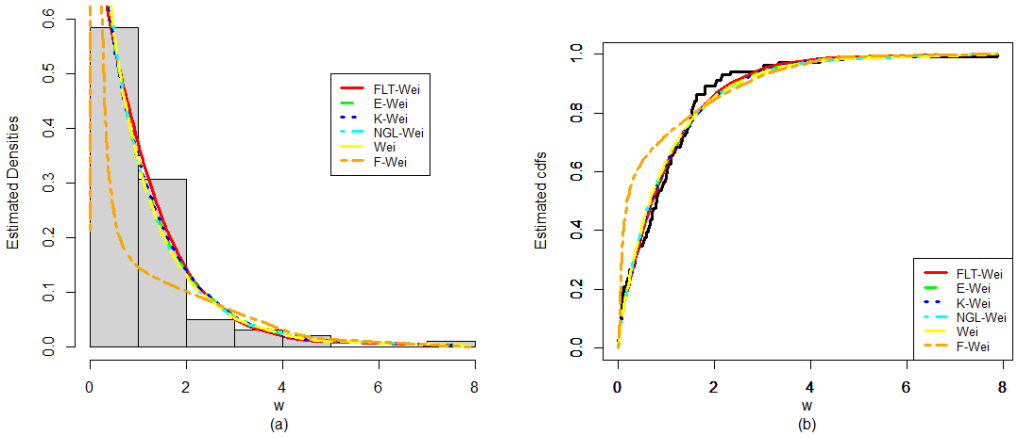

Figure 9. The graphical illustration of the (a) estimated PDFs, (b) estimated CDFs of the fitted distributions for DS 1.

Table 4. The numerical values of the model adequacy measures of the fitted distributions for DS1.

Models	AIC	BIC	CAIC	HQAIC	CRMI	ANDA	KOSA	P-values
FLT-Wei	209.1255	216.9709	209.3729	212.3015	0.1086	0.6864	0.0646	0.7930
E-Wei	211.5743	219.4197	211.8218	214.7504	0.1652	0.9586	0.0844	0.4680
K-Wei	213.2550	223.7155	213.6717	217.4897	0.1439	0.8628	0.0778	0.5745
NGL-Wei	211.9445	219.7899	212.1920	215.1206	0.1974	1.1053	0.0908	0.3763
Wei	210.9536	217.1839	210.0761	213.0710	0.1987	1.1111	0.0906	0.3778
F-Wei	276.4215	281.6517	276.544	278.5389	1.10544	5.96052	0.30684	1.1e-08

1.48, 1.48, 1.49,1.49, 1.50, 1.50, 1.51, 1.52, 1.53, 1.54, 1.55, 1.55, 1.58, 1.59, 1.60, 1.61,1.61, 1.61, 1.61,1.62, 1.62, 1.63, 1.64, 1.66, 1.66, 1.66, 1.67, 1.68, 1.68, 1.69, 1.70, 1.70, 1.73,1.76, 1.76,1.77, 1.78, 1.81, 1.82, 1.84, 1.84, 1.89, 2.00, 2.01, 2.24.

For DS2, some key descriptive measures are min.= 0.55, Q1 (1^{st} quartile)=1.375, median=1.59, mean=1.507, Q3 (3^{rd} quartile) = 1.685, max.= 2.240, skewness=-0.8999, kurtosis=3.9238, variance=0.1051, and range=1.69. Furthermore, for DS 2, some basic plots including the Box plot, Violin plot, and TTT plot are sketched in Figure 10.

Link to DS 2, the values of MLEs of the fitted models (i.e. $\hat{\delta}_{MLE}$, $\hat{\phi}_{MLE}$, $\hat{\beta}_{MLE}$, $\hat{a}_{MLE}$, and $\hat{b}_{MLE}$) are recorded in Table 5. Furthermore, Figure 11 illustrates the profile-log-likelihood function plots of $\hat{\delta}_{MLE}$, $\hat{\phi}_{MLE}$, and $\hat{\beta}_{MLE}$of the NLT-Wei distribution. From Figure 11, we can see that the estimated parameters are maximization of the Log-LF of the NLT-Wei model.

Using DS 2, the AIC, BIC, CAIC, HQAIC, CRMI, ANDA, KOSA, and P-Values of the FLT-Wei and competing distributions are presented in Table 6. For the NLT-Wei model, these values are AIC=30.8505, BIC=37.2799, CAIC=31.2573, HQIC=33.3792, CRMI=0.1222, ANDA=0.6828, KOSA=0.1166, and P-value= 0.3587. Thus, Table 6, categorically confirms that the AIC, BIC, CAIC, HQAIC, CRMI, ANDA, and KOSA values are minimum and the P-value is the maximum of the NLT-

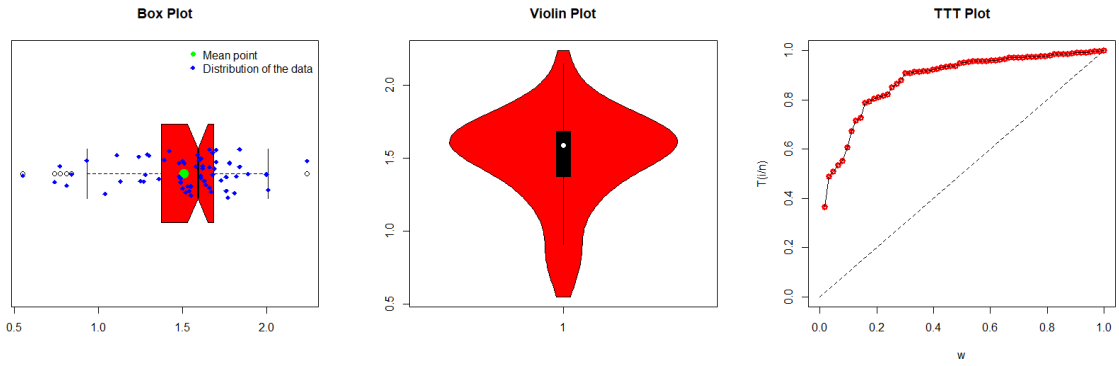

Figure 10. The Box, violin, and TTT plots for the DS2.

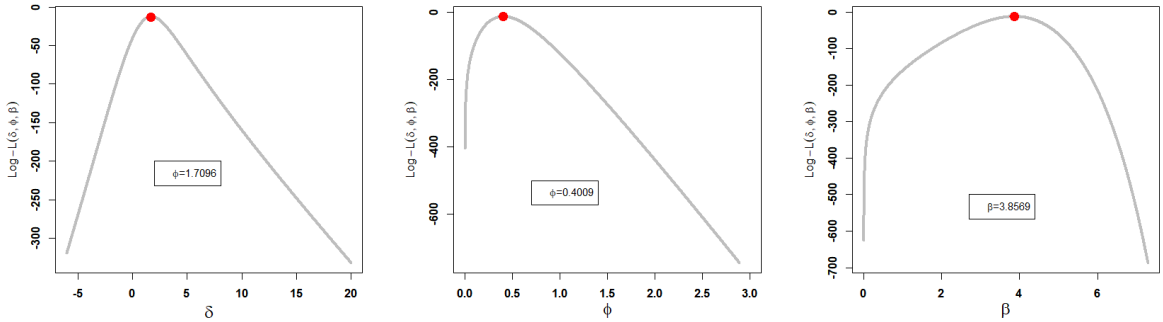

Figure 11. The profile log-likelihood plots for $\hat{\delta}_{MLE}$, $\hat{\phi}_{MLE}$, and$\hat{\beta}_{MLE}$of the NLT-Wei distribution using DS 2.

Wei distribution for DS 2 against the other compared distributions. Therefore, it is concluded that the NLT-Wei model also provides the first-ranked fit to the DS 2. Similarly, supporting numerical results (or illustrations) recorded in Table 6, we also show the graphical display of the NLT-Wei distribution for DS 2. For graphical illustration, we select the estimated PDFs, and estimated CDFs of the proposed and other competitive distributions; see Figure 12. From Figure 12, we can also see the close-fitting ability of the NLT-Wei distribution.

Table 5. For DS 2, the values $\hat{\delta}_{MLE}$, $\hat{\phi}_{MLE}$, $\hat{\beta}_{MLE}$, $\hat{a}_{MLE}$, and $\hat{b}_{MLE}$.

Models	$\hat{\delta}_{MLE}$	$\hat{\phi}_{MLE}$	$\hat{\beta}_{MLE}$	$\hat{a}_{MLE}$	$\hat{b}_{MLE}$
FLT-Wei	1.7096	0.4009	3.8569	-	-
E-Wei	0.6813	0.0204	7.2123	-	-
K-Wei	-	0.1110	7.1056	0.5098	0.2238
NGL-Wei	0.2935	0.0719	5.5546	-	-
Wei	-	0.0599	5.7763	-	-
F-Wei	-	1.7097	4.4915	-	-

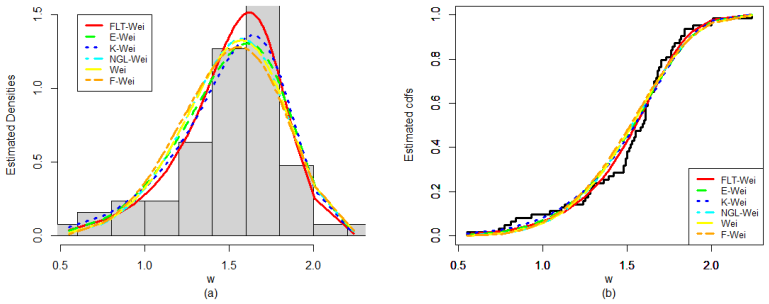

Figure 12. The graphical illustration of the (a) estimated PDFs, (b) estimated CDFs of the fitted distributions for DS 2.

Table 6. Model adequacy measures of the fitted distributions for DS 2.

Models	**AIC**	**BIC**	**CAIC**	**HQAIC**	**CRMI**	**ANDA**	**KOSA**	**P-values**
FLT-Wei	30.8505	37.2799	31.2573	33.3792	0.1222	0.6828	0.1166	0.3587
E-Wei	35.3529	41.7823	35.7597	37.8816	0.2010	1.1168	0.1470	0.1314
K-Wei	35.5131	44.0857	36.2028	38.8848	0.1493	0.8478	0.1338	0.2094
NGL-Wei	36.3771	42.8065	36.7838	38.9058	0.2372	1.3031	0.1513	0.1117
Wei	34.4137	38.7001	34.6137	36.0996	0.2374	1.3045	0.1525	0.1069
F-Wei	36.5999	40.8861	36.7999	38.2857	0.2851	1.5592	0.1676	0.0581

6.3. Application III

In this third sub-section, we offer the third evaluation of the NLT-Wei distribution with other competing well-known distributions by using DS 3. The DS 3 represents impregnated 1000-carbon fiber tows single-carbon fibers and for reader interest, the DS 3 is given by: 0.0312, 0.314, 0.479, 0.552, 0.700, 0.803, 0.861, 0.865, 0.944, 0.958, 0.966, 0.977, 1.006, 1.021, 1.027, 1.055, 1.063, 1.098, 1.140, 1.179, 1.224, 1.240, 1.253, 1.270, 1.272, 1.274, 1.301, 1.301, 1.359, 1.382, 1.382, 1.426, 1.434, 1.435, 1.478, 1.490, 1.511, 1.514, 1.535, 1.554, 1.566, 1.570, 1.586, 1.629, 1.633, 1.642, 1.648, 1.684, 1.697, 1.726, 1.770, 1.773, 1.800, 1.809, 1.818, 1.821, 1.848, 1.880, 1.954, 2.012, 2.067, 2.084, 2.090, 2.096, 2.128, 2.233, 2.433, 2.585, 2.585.

Corresponding to DS 3, some basic descriptive measures are: min.= 0.0312, Q1 (1^{st} quartile). = 1.0980, median=1.4780, mean=1.447, Q3 (3^{rd} quartile). = 1.773, max.= 2.585, skewness=-0.1603, kurtosis=3.2356, variance=0.2559, and range=2.5538. Furthermore, for DS 4, some basic plots including the Box plot, Violin plot, and TTT-plot are displayed in Figure 13.

Link to DS 3, the values of MLEs of the fitted models (i.e. $\hat{\delta}_{MLE}$, $\hat{\phi}_{MLE}$, $\hat{\beta}_{MLE}$, $\hat{a}_{MLE}$, and $\hat{b}_{MLE}$) are recorded in Table 7. Furthermore, Figure 14 illustrates the profile log-likelihood function plots of $\hat{\delta}_{MLE}$, $\hat{\phi}_{MLE}$, and $\hat{\beta}_{MLE}$of the NLT-Wei distribution. From Figure 14, we can clearly see that the estimated parameters are maximization of the Log-LF of the NLT-Wei model.

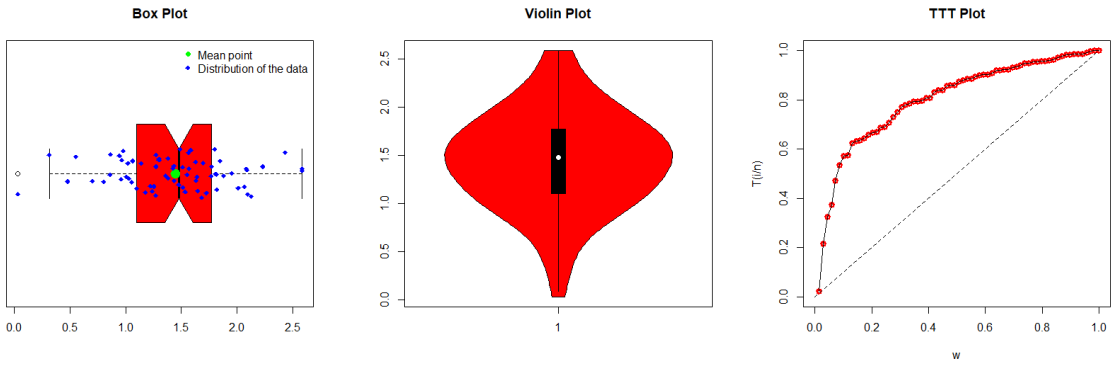

Figure 13. The Box plot, violin plot, and TTT plot for the DS3.

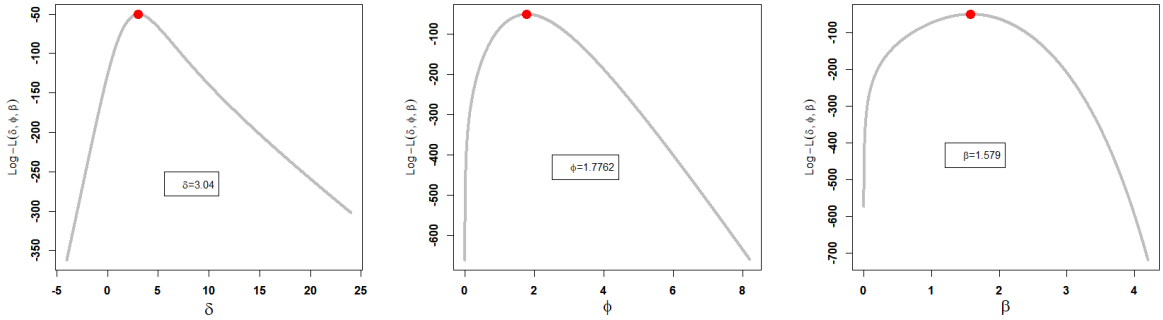

Figure 14. The profile log-likelihood plots for$\hat{\delta}_{MLE}$, $\hat{\phi}_{MLE}$, and$\hat{\beta}_{MLE}$of the NLT-Wei distribution using DS 3.

Using DS 3, the AIC, BIC, CAIC, HQAIC, CRMI, ANDA, KOSA, and P-Values of the NLT-Wei and competing distributions are provided in Table 8. For the NLT-Wei distribution, these values are AIC=107.0333, BIC=113.7356, CAIC=107.4025, HQIC=109.6923, CRMI=0.0271, ANDA=0.2304, KOSA=0.0475, and P-value= 0.9977. Thus, Table 8 confirms that the AIC, BIC, CAIC, HQAIC, CRMI, ANDA, and KOSA values are minimum and the P-value is the maximum of the NLT-Wei distribution for DS 3 against the other compared distributions. Therefore, it is concluded that the NLT-Wei distribution provides the first-ranked fit to the DS 3. Similarly, supporting numerical results recorded in Table 8, we also show the graphical illustration (or visual illustration) of the NLT-Wei distribution for DS 3. Furthermore, for graphical illustration, we select the estimated PDFs, and estimated CDFs plots of the proposed and other competing distributions; see Figure 15. From Figure 15, we can also see the close-fitting ability of the NLT-Wei model as compared to the other competitive distributions.

Table 7. For DS 3, the values $\hat{\delta}_{MLE}$, $\hat{\phi}_{MLE}$, $\hat{\beta}_{MLE}$, $\hat{a}_{MLE}$, and $\hat{b}_{MLE}$.

Models	$\hat{\delta}_{MLE}$	$\hat{\phi}_{MLE}$	$\hat{\beta}_{MLE}$	$\hat{a}_{MLE}$	$\hat{b}_{MLE}$
FLT-Wei	3.0400	1.7763	1.5790	-	-
E-Wei	0.5243	0.0585	4.5293	-	-
K-Wei		0.7842	3.8903	0.3895	0.1569
NGL-Wei	0.8598	0.3363	2.7185	-	-
Wei	-	0.2380	3.0393	-	-
F-Wei	-	0.6533	1.1107	-	-

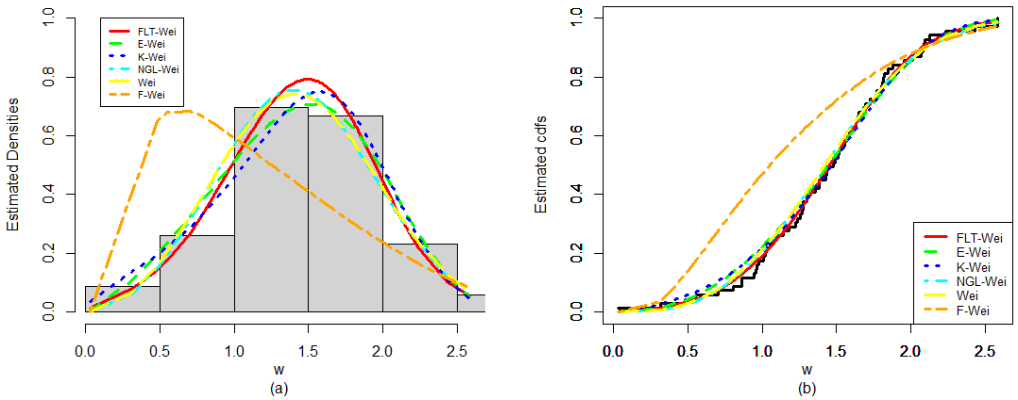

Figure 15. The graphical illustration of the (a) estimated PDFs, and (b) estimated CDFs plots of the fitted distributions for DS 3.

Table 8. Model adequacy (or analytical) measures of the fitted distributions for DS 3.

Models	**AIC**	**BIC**	**CAIC**	**HQIC**	**CRMI**	**ANDA**	**KOSA**	**P-values**
FLT-Wei	107.0333	113.7356	107.4025	109.6923	0.0271	0.2304	0.0475	0.9977
E-Wei	111.3913	118.0937	111.7606	114.0504	0.0710	0.5365	0.0787	0.7868
K-Wei	110.3631	119.2995	110.9881	113.9085	0.0491	0.3872	0.0759	0.8215
NGL-Wei	113.6128	120.3151	113.982	116.2718	0.0794	0.5815	0.0624	0.9510
Wei	111.9152	116.3834	112.0971	113.6879	0.0831	0.6075	0.0661	0.9239
F-Wei	191.8296	196.2978	192.0114	193.6023	0.9495	5.6656	0.3193	1.56e-06

7. Concluding remarks

This paper suggested a novel distribution approach based on logarithmic and trigonometric functions. The newly developed approach may be called a New Logarithmic Tangent-U family of probability distributions, and it can be used to enhance the flexibility level of the existing distributions by adding only one extra parameter. The Weibull model is used as a base member of the NLT-U method of probability distributions and proposed a new probability distribution. The new probability distribution is very flexible and called a New Logarithmic Tangent Weibull (NLT-Wei) model. To illustrate the flexibility of the proposed distribution, the corresponding CDF, SF, PDF, and HF are also graphically visualized in the manuscript. The PDF graphs of the NLT-Wei distribution can take three behaviors right skewed, left skewed, and symmetric shapes. Similarly, the HF graphs of the NLT-Wei distribution can take unimodal, increasing-decreasing-increasing unimodal, increasing, decreasing, and bathtub shapes. Some fundamental properties of the NLT-U family of distributions are investigated in detail. The MLE approach is utilized to estimate the unknown model parameters of the NLT-U family of distributions. To judge the effectiveness of the estimated parameters procedure (or MLE method), a MCSS is conducted, which reveals that as the sample size upsurges the biases and MSEs decline. The simulation results are presented numerically as well as graphically. After fundamental properties and simulation analysis, the practical performance of the NLT-Wei distribution is illustrated by considering three real data sets from the field of engineering. The optimization (or practical applications) of the NLT-Wei distribution is compared with Exponentiated Weibull, Kumaraswamy Weibull, New Generalized Logarithmic Weibull, Weibull, and Flexible Weibull distributions. Based on goodness-of-fit measures, p-values, and other graphical illustrations, it is observed that the NLT-Wei distribution performs better than other competing distributions. Further, we strongly hope that this new development will be valuable in future.

References

1. Alghamdi, S. M., Shrahili, M., Hassan, A. S., Gemeay, A. M., Elbatal, I., & Elgarhy, M. (2023). Statistical inference of the half logistic modified Kies exponential model with modeling to engineering data. *Symmetry*, *15*(3), 586.
2. Tashkandy, Y. A., Nagy, M., Akbar, M., Mahmood, Z., Gemeay, A. M., Hossain, M. M., & Muse, A. H. (2023). The Exponentiated Cotangent Generalized Distributions: Characteristics and Applications Patients of Chemotherapy Treatments Data. *IEEE Access*.
3. Alsadat, N., Ahmad, A., Jallal, M., Gemeay, A. M., Meraou, M. A., Hussam, E., ... & Hossain, M. M. (2023). The novel Kumaraswamy power Frechet distribution with data analysis related to diverse scientific areas. *Alexandria Engineering Journal*, *70*, 651-664.
4. Gómez, Y. M., Gallardo, D. I., Bourguignon, M., Bertolli, E., & Calsavara, V. F. (2023). A general class of promotion time cure rate models with a new biological interpretation. *Lifetime Data Analysis*, *29*(1), 66-86.
5. Odhah, O. H., Alshanbari, H. M., Ahmad, Z., & Rao, G. S. (2023). A weighted cosine-G family of distributions: properties and illustration using time-to-event data. *Axioms*, *12*(9), 849.

6. Mudholkar, G. S., & Srivastava, D. K. (1993). Exponentiated Weibull family for analyzing bathtub failure-rate data. IEEE transactions on reliability, 42(2), 299-302.
7. Marshall AW, Olkin I. A new method for adding a parameter to a family of distributions with application to the exponential and Weibull families. Biometrika. 1997 Sep 1; 84(3):641–52.
8. Gupta, R. D., & Kundu, D. (2001). Exponentiated exponential family: an alternative to gamma and Weibull distributions. *Biometrical Journal: Journal of Mathematical Methods in Biosciences*, *43*(1), 117-130.
9. Eugene, N., Lee, C., & Famoye, F. (2002). Beta-normal distribution and its applications. *Communications in Statistics-Theory and methods*, *31*(4), 497-512.
10. Nadarajah, S., Cordeiro, G. M., & Ortega, E. M. (2012). General results for the Kumaraswamy-G distribution. *Journal of Statistical Computation and Simulation*, *82*(7), 951-979.
11. Chesneau, C., Bakouch, H. S., & Hussain, T. (2019). A new class of probability distributions via cosine and sine functions with applications. *Communications in Statistics-Simulation and Computation*, *48*(8), 2287-2300.
12. Souza, L., Junior, W., De Brito, C., Chesneau, C., Ferreira, T., & Soares, L. (2019). On the Sin-G class of distributions: theory, model and application. *Journal of Mathematical Modeling*, *7*(3), 357-379.
13. Silveira F., Gomes-Silva F., Brito C., Cunha-Filho M., Jale J., Gusmao F., et al. (2020). The normal-tangent-G class of probabilistic distributions: properties and real data modeling. Pakistan Journal of Statistics and Operation Research, 16, 827–838.
14. Alotaibi, N., Al-Moisheer, A. S., Elbatal, I., Elgarhy, M., & Almetwally, E. M. Bayesian and Non-Bayesian Analysis for the Sine Generalized Linear Exponential Model under Progressively Censored Data. Computer Modeling in Engineering & Sciences, 140(3), 2795-2823
15. Nanga, S., Nasiru, S., & Dioggban, J. (2022). Tangent Topp-Leone family of distributions. Scientific African, *17*, e01363.
16. Zaidi, S. M., Mahmood, Z., Atchadé, M. N., Tashkandy, Y. A., Bakr, M. E., Almetwally, E. M., ... & Kumar, A. (2024). Lomax tangent generalized family of distributions: characteristics, simulations, and applications on hydrological-strength data. Heliyon.
17. Zhao, Y., Ahmad, Z., Alrumayh, A., Yusuf, M., Aldallal, R., Elshenawy, A., & Riad, F. H. (2023). A novel logarithmic approach to generate new probability distributions for data modeling in the engineering sector. *Alexandria Engineering Journal*, *62*, 313-325.
18. Ahmad, A., Rather, A. A., Tashkandy, Y. A., Bakr, M. E., El-Din, M. M. M., Gemeay, A. M., ... & Salem, M. (2024). Deriving the new cotangent Fréchet distribution with real data analysis. Alexandria Engineering Journal, 105, 12-24.
19. Muhammad, M., Bantan, R. A., Liu, L., Chesneau, C., Tahir, M. H., Jamal, F., & Elgarhy, M. (2021). A new extended cosine—G distributions for lifetime studies. *Mathematics*, *9*(21), 2758.
20. Alomair, M. A., Ahmad, Z., Rao, G. S., Al-Mofleh, H., Khosa, S. K., & Al Naim, A. S. (2023). A new trigonometric modification of the Weibull distribution: Control chart and applications in quality control. *Plos one*, *18*(7), e0286593.

21. Kamal, M., Rao, G. S., Alsolmi, M. M., Ahmad, Z., Aldallal, R., & Rahman, M. M. (2023). A new statistical methodology using the sine function: Control chart with an application to survival times data. *Plos one*, *18*(8), e0285914.
22. Benchiha, S., Sapkota, L. P., Al Mutairi, A., Kumar, V., Khashab, R. H., Gemeay, A. M., ... & Nassr, S. G. (2023). A new sine family of generalized distributions: Statistical inference with applications. *Mathematical and Computational Applications*, *28*(4), 83.
23. Cordeiro, G. M., Ortega, E. M., & Nadarajah, S. (2010). The Kumaraswamy Weibull distribution with application to failure data. Journal of the Franklin Institute, 347(8), 1399-1429.
24. Weibull, W. (1951). A statistical distribution function of wide applicability. *Journal of applied mechanics*.
25. Bebbington, M., Lai, C. D., & Zitikis, R. (2007). A flexible Weibull extension. *Reliability Engineering & System Safety*, *92*(6), 719-726.
26. Shah, Z., Khan, D. M., Khan, Z., Faiz, N., Hussain, S., Anwar, A., ... & Kim, K. I. (2023). A New Generalized Logarithmic–X Family of Distributions with Biomedical Data Analysis. *Applied Sciences*, *13*(6), 3668.
27. Chamunorwa, S., Makubate, B., Oluyede, B., & Chipepa, F. (2021). The exponentiated half logistic-log-logistic Weibull distribution: Model, properties and applications. *Journal of Statistical Modelling: Theory and Applications*, *2*(1), 101-120.
28. Dey, S., Sharma, V. K., & Mesfioui, M. (2017). A new extension of Weibull distribution with application to lifetime data. *Annals of Data Science*, *4*, 31-61.
29. Nagarjuna, V. B., Vardhan, R. V., & Chesneau, C. (2021). Kumaraswamy generalized power Lomax distribution and its applications. *Stats*, *4*(1), 28-45.